EDGE ARTICLE

Check for updates

Unusual fcc-structured Ag₁₀ kernels trapped in Ag₇₀ nanoclusters†

Yan-Min Su,‡[a] Zhi Wang,‡[a] Gui-Lin Zhuang, [ID][b] Quan-Qin Zhao,[a] Xing-Po Wang,[a] Chen-Ho Tung[a] and Di Sun [ID]*[a]

Controlled trapping atom-precise ultrasmall silver nanoparticles into silver nanoclusters is challenging; thus only limited progress has been made in this area. We are therefore inspired to isolate two novel silver nanoclusters, Ag₁₀@Ag₇₀ (**SD/Ag80a** and **SD/Ag80b**; SD = SunDi), where a novel fcc-structured Ag₁₀ kernel built from two single-edge opened Ag₆ octahedra by sharing one edge is trapped. The bioctahedral Ag₁₀ kernel is locked by a pair of $Mo_7O_{26}^{10-}$ anions to form an inner Ag₁₀@(Mo₇O₂₆)₂ core which is further encapsulated by an outer Ag₇₀ shell to form three-shell Ag₁₀@(Mo₇O₂₆)₂@Ag₇₀ nanoclusters. Notably, the bioctahedral Ag₁₀ kernel has not been observed in silver nanoclusters ever before, thus representing a new embryo state of silver nanoparticles. **SD/Ag80a** emits in the near infrared (NIR) region (λ_{em} = 730 nm) at low temperature. This work will deepen our understanding on the atomic-level growth of silver nanoparticles and complicated three-shell self-assembly involving polyoxometalate (POM) and two different silver nanoclusters.

Introduction

Ultrasmall silver nanoparticles (*e.g.*, few-atom clusters, <1 nm) represent the embryo states of larger silver nanoparticles (typically >2 nm) to some extent, which have defined molecular structures and compositions and thus can deepen the understanding on the size evolution of silver nanoparticles.[1] Given this, X-ray single crystal structures become a prerequisite to get atomic-level information including the surface ligands, inorganic–organic interfaces and silver atoms packed in silver nanoparticles.[2] While chasing large silver nanoclusters such as Ag₁₄, Ag₂₁, Ag₂₃, Ag₄₄, Ag₅₀, Ag₆₂, Ag₆₇, Ag₇₄, and Ag₁₄₁ and even the largest known Ag₃₇₄,[3] chemists almost neglect the significance of the embryo states of silver nanoparticles that however are quite difficult to be captured due to their typical kinetics-controlled growth course.[4] Therefore, controlling the reductive transformation from Ag(ɪ) to Ag⁰ and then trapping the transient Ag aggregates into the thermodynamically stable crystalline product during the self-assembly is an urgent need and thus a major challenge.

Learning from the solvent-controlled synthesis of multiple-twin decahedral and icosahedral silver nanoparticles with special favourable [111] facets,[5] we found that DMF (*N,N*-dimethylformamide), compared to widely used NaBH₄, is a much more mild reductive agent which facilitates the formation of Ag₆ octahedral kernels during the slow reduction process as seen in Ag₃₄ and Ag₆₂ nanoclusters.[6] Such Ag₆ octahedra can be seen as the smallest fragment cut from the unit cell of face-centered cubic (fcc) bulk silver metal, whereas other silver nanoclusters smaller than the most common icosahedral Ag₁₃ are still not directly observed in any reported silver nanoclusters.[7] Thus, the species in the early evolution from discrete Ag atoms to the metallic state are still largely vague and the exploration of a suitable synthesis strategy to trap them is scientifically desired.

With these considerations in mind, we used a DMF-containing mixed solvent system to isolate two novel silver nanoclusters [Ag₁₀@(Mo₇O₂₆)₂@Ag₇₀(MoO₄)₂(CyhS)₃₆(CF₃SO₃)₁₆(DMF)₆]·2DMF·4ⁿPrOH (**SD/Ag80a**; SD = SunDi; CyhSH = cyclohexanethiol) and [Ag₁₀@(Mo₇O₂₆)₂@Ag₇₀(MoO₄)₂(ⁱPrS)₃₆(CF₃SO₃)₁₆(DMF)₆] (**SD/Ag80b**). Two silver nanoclusters have the same metallic core but different organic coatings. In the innermost of cluster, an unusual fcc-structured Ag₁₀ nanocluster constructed from two single-edge opened Ag₆ octahedra by sharing one edge is locked by a pair of $Mo_7O_{26}^{10-}$ anions to form an inner Ag₁₀@(Mo₇O₂₆)₂ core which acts as a template to support the outer Ag₇₀ nanocluster to form a final three-shell Ag₁₀@(Mo₇O₂₆)₂@Ag₇₀ nanocluster. This unprecedented bioctahedral Ag₁₀ nanocrystal can be deemed as a new nanofragment cut from fcc silver metal and represents a possible transient species in the growth of large silver nanoparticles.

[a]*Key Lab for Colloid and Interface Chemistry of Education Ministry, School of Chemistry and Chemical Engineering, Shandong University, Jinan, 250100, People's Republic of China. E-mail: dsun@sdu.edu.cn*

[b]*College of Chemical Engineering and Materials Science, Zhejiang University of Technology, Hangzhou, 310032, People's Republic of China*

† Electronic supplementary information (ESI) available: IR, ¹³C NMR, CV, UV, EDS, PXRD and luminescence decay curve, and details of the data collection and structure refinements, and crystal data. CCDC 1850394 and 1850395 for **SD/Ag80a** and **SD/Ag80b**. For ESI and crystallographic data in CIF or other electronic format see DOI: 10.1039/c8sc03396j

‡ These authors contributed equally.

Results and discussion

X-ray structures of SD/Ag80a and SD/Ag80b

SD/Ag80a and **SD/Ag80b** were synthesized through a facile one-pot solvothermal reaction of silver-thiolate polymeric precursors, CF_3SO_3Ag and molybdates in different DMF-containing mixed solvent systems (Scheme 1). In spite of several attempts, we still couldn't isolate **SD/Ag80a** and **SD/Ag80b** using the same Mo sources. Their samples were collected as brown-yellow and red crystals, respectively, after evaporation of solvents at room temperature for 1–2 weeks. Several synthetic parameters were optimized and are listed in Tables S1 and S2 (ESI)† for details. Details of the synthesis and some basic characterization are shown in the ESI.†

The molecular structures of **SD/Ag80a** and **SD/Ag80b** were revealed by single-crystal X-ray diffraction (SCXRD) analysis. They crystallize in monoclinic $P2_1/n$ and triclinic $P\bar{1}$ space groups, respectively. In each asymmetric unit only half of the corresponding clusters were resolved. Due to the structural similarities, only that of **SD/Ag80a** is described in detail here. The structural diagrams of **SD/Ag80b** are shown in Fig. S1.† Selected details of the data collection and structure refinements are listed in Table S3.†

SD/Ag80a is an elongated spheroid ($1.0 \times 1.4 \times 2.1$ nm) that sits on the crystallographic inversion center (i). The Ag_{80} nanocluster is composed of a Ag_{70} shell and a Ag_{10} kernel. The Ag_{70} shell is capped by 36 CyhS$^-$, 16 CF$_3$SO$_3^-$, 2 MoO$_4^{2-}$ and 6 DMF (Fig. 1a and b). All cyclohexyl groups of 36 CyhS$^-$ ligands show a unified chair configuration. Two different coordination modes (μ_3 and μ_4) are found in 36 CyhS$^-$ ligands capped on the silver trigons or tetragons (Ag–S distances: 2.389(5)–2.722(5) Å). The 16 CF$_3$SO$_3^-$ anions exhibit three different coordination fashions including μ_3-η^1:η^2:η^0, μ_3-η^1:η^1:η^1, and μ_2-η^1:η^1:η^0. Two MoO$_4^{2-}$ anions (yellow tetrahedra in Fig. 1) adopt a μ_8-η^2:η^3:η^3 mode to bind in the equatorial region of the Ag_{70} shell. Six DMF molecules as terminal ligands finished the organic ligand coverage on the surface of the Ag_{70} shell. Three different O donor ligands (CF$_3$SO$_3^-$, MoO$_4^{2-}$, and DMF) interact with Ag atoms with the bonding distances in the ranges of 2.406(15)–2.789(17), 2.251(11)–2.568(11) and 2.390(13)–2.458(14) Å, respectively. The Ag_{70} shell was further consolidated by the argentophilic interaction[8] ranging from 2.833(2) to 3.4394(16) Å. The surface of the Ag_{70} shell consists silver trigons, tetragons, pentagons and heptagons (Fig. 1c). The silver trigons, tetragons,
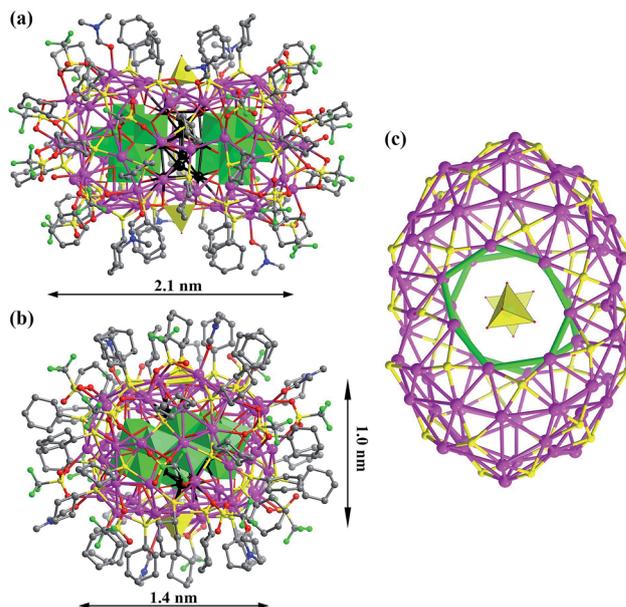

Fig. 1 (a) and (b) The X-ray crystal structure of $Ag_{10}@(Mo_7O_{26})_2@Ag_{70}$ nanoclusters viewed along two orthogonal directions. The inner silver atoms of the Ag_{10} kernel are highlighted in black. $Mo_7O_{26}^{10-}$ and MoO_4^{2-} are represented by green and yellow polyhedra, respectively. (c) The $Ag_{70}S_{36}$ shell with silver heptagons highlighted in green.

and pentagons are capped by CyhS$^-$ or CF$_3$SO$_3^-$, whereas MoO$_4^{2-}$ shapes the large silver heptagons (green rings in Fig. 1c).

There are two crescent-like $Mo_7O_{26}^{10-}$ anions under the Ag_{70} shell (Fig. 2a). During the synthesis of **SD/Ag80a** and **SD/Ag80b**, although different Mo sources, Na$_2$MoO$_4$·2H$_2$O and [(^{n}Bu$_4$N)$_2$-Mo$_6$O$_{19}$], were used, respectively, the same $Mo_7O_{26}^{10-}$ anion was trapped as the template in the final silver nanoclusters. Thus, the novel $Mo_7O_{26}^{10-}$ anions should be *in situ* transformed from Na$_2$MoO$_4$·2H$_2$O or [(^{n}Bu$_4$N)$_2$(Mo$_6$O$_{19}$)] in different solvent environments. We used Bond-Valence Sum (BVS) calculations for seven Mo atoms of $Mo_7O_{26}^{10-}$, which confirmed that all of them are in the +6 oxidation state (Table S5†).[9] The $Mo_7O_{26}^{10-}$ is constructed from seven edge-shared MoO$_6$ octahedra. The total 26 O atoms are divided into four kinds based on their binding fashion to Ag atoms, 2 μ_0, 4 μ_1, 16 μ_2, and 4 μ_3. Such highly negative-charged $Mo_7O_{26}^{10-}$ totally binds 35 silver atoms. Among them, 7 are from the inner Ag_{10} kernel and the remaining 28 are from the Ag_{70} shell (Fig. 2b). Notably, this novel molybdate has neither been observed in classic POM chemistry nor in silver nanoclusters. More importantly, this molybdate carries the second highest negative charges[10] which effectively enhanced its template effect by binding more Ag atoms (Table S6†).

The most interesting feature in **SD/Ag80a** is the unusual Ag_{10} kernel underlying the equatorial region of the Ag_{70} shell which is built from two single-edge opened Ag_6 octahedra by sharing one edge (Fig. 2c). The shared edge is the longest Ag···Ag edge (Ag38···Ag38^i = 3.457(1) Å, symmetry code i: $-x + 1$, $-y + 1$, $-z + 1$) within the Ag_{10} kernel, which is out of the normal Ag···Ag interaction range. All other eleven Ag···Ag edges are
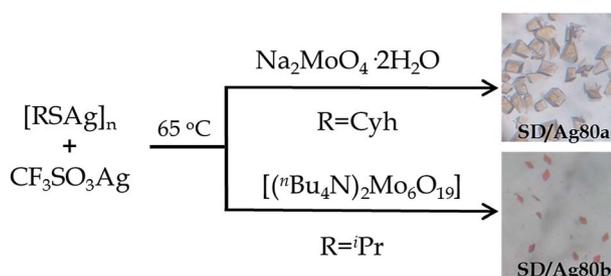
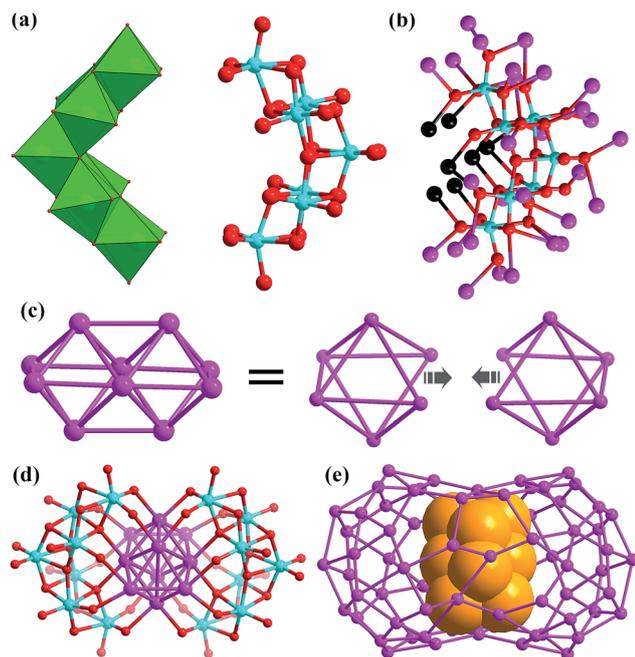

Scheme 1 Synthetic routes for **SD/Ag80a** and **SD/Ag80b**.

Fig. 2 (a) Two $Mo_7O_{26}^{10-}$ anions in **SD/Ag80a** shown in polyhedral (left) and ball-and-stick modes (right). (b) Binding fashion of $Mo_7O_{26}^{10-}$ toward 35 Ag atoms (black: Ag from the Ag_{10} kernel; purple: Ag from the Ag_{70} shell). (c) Animation showing the formation of a Ag_{10} bioctahedron from two single-edge opened Ag_6 octahedra by fusing one Ag–Ag edge. (d) The Ag_{10} bioctahedron locked by a pair of $Mo_7O_{26}^{10-}$ anions. (e) The Ag_{10} bioctahedron (claybank space-filling balls) residing in the Ag_{70} shell.

distributed in the range of 2.659(2)–2.980(1) Å (Fig. S2†) and the average Ag⋯Ag distance is 2.814 Å, which is 2.5% shorter than the Ag⋯Ag distance in metallic silver (2.886 Å),[11] indicating strong argentophilic interactions as in bulk silver metal. All exposed trigons of the Ag_{10} bioctahedral kernel are [111] facets which are capped by $Mo_7O_{26}^{10-}$ anions through Ag–O bonding (Ag–O distances: 2.284(10)–2.433(10) Å; Fig. 2d). As such, the Ag_{10} bioctahedron is doubly clamped by a pair of $Mo_7O_{26}^{10-}$ anions to form an inner $Ag_{10}@(Mo_7O_{26})_2$ core, which was enwrapped by an outer Ag_{70} shell to form a three-shell $Ag_{10}@(Mo_7O_{26})_2@Ag_{70}$ nanocluster. The two polar sites of the Ag_{10} bioctahedron are also linked with the outer Ag_{70} shell through argentophilic interactions (Ag⋯Ag: 2.8523(19)–3.3621(18) Å; Fig. S3†).

Although the single Ag_6 octahedron has been observed in several inorganic compounds[12] and a few silver nanoclusters,[13] its dimer, Ag_{10} bioctahedron, has never been observed before in silver nanoclusters. Such a Ag_{10} bioctahedron can be seen as a bigger nanofragment than a Ag_6 octahedron. An important driven force for its formation should be the suitable reducibility of DMF.[6] The oxidation product of DMF in the assembly process is Me_2NCOOH[14] which can be recognized from the ^{13}C NMR (nuclear magnetic resonance) of HCl digested reaction mother solution (Fig. S4†). In the chemical shift scale corresponding to aldehydes and carboxylates (δ = 150–200 ppm), two peaks appeared at δ = 164.64 and 162.92 ppm, which are assigned to the carbon resonances of DMF and Me_2NCOOH, respectively.

We didn't observe any peaks in ^{13}C NMR corresponding to the oxidation product of ^nPrOH, which clearly excluded the possible reductive effect of ^nPrOH in this assembly system. These results clearly evidenced the redox reaction between Ag(I) and DMF occurred during the self-assembly process. The emergence of a fcc-structured Ag_{10} nanocluster, on the other hand, answered an important question, which is how the common observed smaller Ag_6 kernel grew up to larger structures. Based on the above structural information, we can tentatively assign a new edge-fusion mode to its growth mechanism, although several other growth modes for noble metal nanoparticles have been proposed such as face-fusion, interpenetration, shell-by-shell, layer-by-layer, and tetrahedron-based vertex-sharing growth modes.[2] Based on the formulae and charge neutrality considerations, we can determine that the valence of the Ag_{10} kernel is +6, which means such a kernel carries four free electrons, belonging to a 4e superatom network. We also performed DFT calculations at the B3LYP/SDD theoretical level to study the free electron distributions on the frontier orbitals of the Ag_{10} kernel (see details in the ESI†). According to the results identified experimentally, the inner Ag_{10} kernel features C_i symmetry with +6 valence and four free electrons. Thus, frontier molecular orbital analysis (Fig. S5†) reveals that four free electrons occupy two A_u-symmetry HOMO-1 and HOMO. HOMO-1 and HOMO exhibit different components. HOMO involves in the 5s orbitals of two ends of Ag_{10}, while HOMO-1 concentrates on the 4d orbitals of two ends of Ag_{10}. Moreover, HOMO-2 features A_g symmetry with similar components to HOMO-1, and LUMO consists of 5s orbitals in the centre of Ag_{10}.

Combining the structural analysis and DMF-involved reductive process, we tentatively proposed a total shell-by-shell formation mechanism for such new silver nanoclusters. Weakly reductive DMF firstly induced the formation of an inner Ag_{10} kernel (1st shell), which exposes highly active [111] facets that are quickly passivated by the formation of Ag–O interaction with $Mo_7O_{26}^{10-}$ (2nd shell). The inner $[Ag_{10}@(Mo_7O_{26})_2]$ core acts as the authentic template to support an outer Ag_{70} shell, forming the final core–shell type silver nanoclusters. Such a formation route resembled the mechanism revealed in the $[Ag_6@(MoO_4)_7@Ag_{56}]$ family by electrospray ionization mass spectrometry.[6b]

We also noted that the $Au_{21}(S-Adm)_{15}$ nanocluster has been reported by the Zhu group,[15] who firstly found the bioctahedral Au_{10} kernel formed by edge-sharing of two single-edge opened Au_6 octahedra. However, the shared edge is not the longest one (opened edge) and the overall Au_6 octahedral framework is severely disordered. Anyhow, as a counterpart of this Au_{10} kernel, the bioctahedral Ag_{10} kernel has not been reported before in silver nanoclusters.

The optical properties of SD/Ag80a

The UV/Vis spectrum of **SD/Ag80a** was measured in the solid state using diffuse reflectance mode. As shown in Fig. 3, **SD/Ag80a** showed an absorption maximum at 344 nm and a shoulder peak in the visible region (~490 nm), which should be ascribed to ligand-based absorption and the charge transfer
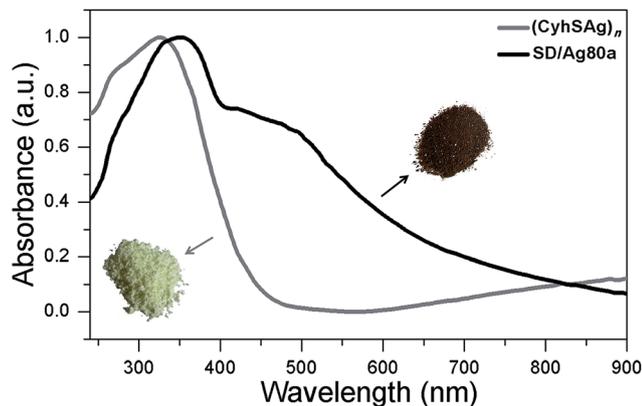
Fig. 3 Optical absorption spectra of **SD/Ag80a** and the silver–thiolate precursor. Insets are photographs of solid samples of **SD/Ag80a** (brown microcrystals) and the polymeric precursor (CyhSAg)$_n$ (pale yellow powder).

transition from the S 3p to Ag 5s orbitals, respectively. Similar assignments were also made in a hypothetical silver sulfide monomer and molecular $[Ag_{62}S_{13}(SBu^t)_{32}]^{4+}$ cluster.[16] Based on the Kubelka–Munk function (Fig. S6†), the band gap of **SD/Ag80a** was estimated to be ~1.06 eV, which indicates that **SD/Ag80a** is a potential narrow-band-gap semiconductor. In comparison, the optical energy gap of the precursor (CyhSAg)$_n$ is ~2.09 eV.

The luminescence properties of **SD/Ag80a** were studied in the solid state. As shown in the insets of Fig. 4, we can observe that **SD/Ag80a** isn't emissive under the UV light irradiation (λ_{ex} = 365 nm) at room temperature; however, it emits red luminescence at 77 K. The varied-temperature emission spectra of **SD/Ag80a** in the solid state were recorded from 293 to 83 K with 30 K as an interval, showing luminescence thermochromic behavior. When gradually cooled to 83 K, the intensity of emission shows an 18-fold enhancement, which should be assigned to the low-temperature induced increase of radiative decay. The emission maximum was blue-shifted from 754 to
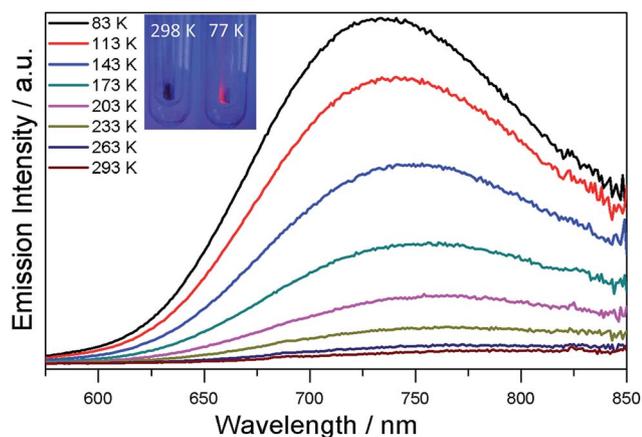
730 nm (λ_{ex} = 469 nm) in the temperature range of 173–83 K (Fig. 4), which may be related to the enhanced molecular rigidity at lower temperature.[17] This near-infrared (NIR) emission should be assigned to ligand-to-metal-charge-transfer (LMCT) transition from S 3p to Ag 5s orbitals.[18] The emission lifetime of **SD/Ag80a**, falling on the microsecond scale at 83 K (Fig. S7†), suggests the triplet phosphorescence origin.

Conclusions

In conclusion, we developed a DMF-controlled strategy to successfully capture an atom-precise ultrasmall Ag$_{10}$ kernel into a gigantic silver nanocluster. The DMF with mild reductive ability plays a key role in the formation of such a novel cluster-in-cluster silver nanocluster. The fcc-structured Ag$_{10}$ kernel is built from two single-edge opened Ag$_6$ octahedra by sharing one edge and further locked by a pair of Mo$_7$O$_{26}$$^{10-}$ anions to form an inner Ag$_{10}$@(Mo$_7$O$_{26}$)$_2$ core which is finally encapsulated by an outer Ag$_{70}$ shell to form three-shell Ag$_{10}$@(Mo$_7$O$_{26}$)$_2$@Ag$_{70}$ nanoclusters. Notably, both the bioctahedral Ag$_{10}$ kernel and crescent-like Mo$_7$O$_{26}$$^{10-}$ have not been observed in silver nanocluster and POM chemistry ever before, respectively. The bioctahedral Ag$_{10}$ core can be deemed as a brand-new embryo state of silver nanoparticles; moreover, it also provides a new edge-fusion growth route for silver nanoparticles from the smallest Ag$_6$ nanofragment of metallic silver. We hope that this work can popularize the new controllable synthetic method to expand the scope of silver nanoclusters with higher complexity.

Conflicts of interest

There are no conflicts to declare.

Acknowledgements

Fig. 4 Varied-temperature luminescence spectra of **SD/Ag80a** from 293–83 K in the solid state. Insets show the photographs of the sample **SD/Ag80a** under a hand-held UV lamp (365 nm) at 298 and 77 K.

References

1 (a) T. U. B. Rao and T. Pradeep, *Angew. Chem., Int. Ed.*, 2010, **49**, 3925–3929; (b) T. U. B. Rao, B. Nataraju and T. Pradeep, *J. Am. Chem. Soc.*, 2010, **132**, 16304–16307; (c) H. Xiang, S.-H. Wei and X. Gong, *J. Am. Chem. Soc.*, 2010, **132**, 7355–7360.

2 (a) R. C. Jin, C. J. Zeng, M. Zhou and Y. X. Chen, *Chem. Rev.*, 2016, **116**, 10346–10413; (b) S. L. Zhuang, L. W. Liao, Y. Zhao, J. Y. Yuan, C. H. Yao, X. Liu, J. Li, H. T. Deng, J. L. Yang and Z. K. Wu, *Chem. Sci.*, 2018, **9**, 2437–2442.

3 (a) H. Yang, J. Lei, B. Wu, Y. Wang, M. Zhou, A. Xia, L. Zheng and N. Zheng, *Chem. Commun.*, 2013, **49**, 300–302; (b) R. S. Dhayal, J.-H. Liao, Y.-C. Liu, M.-H. Chiang, S. Kahlal, J.-Y. Saillard and C. W. Liu, *Angew. Chem., Int. Ed.*, 2015,

54, 3702–3706; (*c*) C. Liu, T. Li, H. Abroshan, Z. M. Li, C. Zhang, H. J. Kim, G. Li and R. C. Jin, *Nat. Commun.*, 2018, **9**, 744; (*d*) A. Desireddy, B. E. Conn, J. Guo, B. Yoon, R. N. Barnett, B. M. Monahan, K. Kirschbaum, W. P. Griffith, R. L. Whetten, U. Landman and T. P. Bigioni, *Nature*, 2013, **501**, 399–402; (*e*) W. J. Du, S. Jin, L. Xiong, M. Chen, J. Zhang, X. J. Zou, Y. Pei, S. X. Wang and M. Z. Zhu, *J. Am. Chem. Soc.*, 2017, **139**, 1618–1624; (*f*) S. Jin, S. X. Wang, Y. B. Song, M. Zhou, J. Zhong, J. Zhang, A. D. Xia, Y. Pei, M. Chen, P. Li and M. Z. Zhu, *J. Am. Chem. Soc.*, 2014, **136**, 15559–15565; (*g*) M. J. Alhilaly, M. S. Bootharaju, C. P. Joshi, T. M. Besong, A.-H. Emwas, R. Juarez-Mosqueda, S. Kaappa, S. Malola, K. Adil, A. Shkurenko, H. Hakkinen, M. Eddaoudi and O. M. Bakr, *J. Am. Chem. Soc.*, 2016, **138**, 14727–14732; (*h*) M. Qu, H. Li, L. H. Xie, S. T. Yan, J. R. Li, J. H. Wang, C. Y. Wei, Y. W. Wu and X. M. Zhang, *J. Am. Chem. Soc.*, 2017, **139**, 12346–12349; (*i*) L. Ren, P. Yuan, H. Su, S. Malola, S. Lin, Z. Tang, B. K. Teo, H. Hakkinen, L. Zheng and N. Zheng, *J. Am. Chem. Soc.*, 2017, **139**, 13288–13291; (*j*) H. Y. Yang, Y. Wang, X. Chen, X. J. Zhao, L. Gu, H. Q. Huang, J. Z. Yan, C. F. Xu, G. Li, J. C. Wu, A. J. Edwards, B. Dittrich, Z. C. Tang, D. D. Wang, L. Lehtovaara, H. Hakkinen and N. F. Zheng, *Nat. Commun.*, 2016, **7**, 12809.

4 (*a*) Y. Wang, Y. Q. Zheng, C. Z. Huang and Y. N. Xia, *J. Am. Chem. Soc.*, 2013, **135**, 1941–1951; (*b*) M. Zhu, P. Wang, N. Yan, X. Q. Chai, L. Z. He, Y. Zhao, N. Xia, C. H. Yao, J. Li, H. T. Deng, Y. Zhu, Y. Pei and Z. K. Wu, *Angew. Chem., Int. Ed.*, 2018, **57**, 4500–4504; (*c*) L. Z. He, J. Y. Yuan, N. Xia, L. W. Liao, X. Liu, Z. B. Gan, C. M. Wang, J. L. Yang and Z. K. Wu, *J. Am. Chem. Soc.*, 2018, **140**, 3487–3490.

5 (*a*) A. Tao, P. Sinsermsuksakul and P. D. Yang, *Angew. Chem., Int. Ed.*, 2006, **45**, 4597–4601; (*b*) M. Tsuji, Y. Maeda, S. Hikino, H. Kumagae, M. Matsunaga, X. L. Tang, R. Matsuo, M. Ogino and P. Jiang, *Cryst. Growth Des.*, 2009, **9**, 4700–4705; (*c*) M. Tsuji, M. Ogino, R. Matsuo, H. Kumagae, S. Hikino, T. Kim and S. H. Yoon, *Cryst. Growth Des.*, 2010, **10**, 296–301; (*d*) M. Tsuji, X. L. Tang, M. Matsunaga, Y. Maeda and M. Watanabe, *Cryst. Growth Des.*, 2010, **10**, 5238–5243.

6 (*a*) D. Sun, G.-G. Luo, N. Zhang, R.-B. Huang and L.-S. Zheng, *Chem. Commun.*, 2011, **47**, 1461–1463; (*b*) Z. Wang, H. F. Su, M. Kurmoo, C. H. Tung, D. Sun and L.-S. Zheng, *Nat. Commun.*, 2018, **9**, 2094.

7 R. S. Dhayal, Y.-R. Lin, J.-H. Liao, Y.-J. Chen, Y.-C. Liu, M.-H. Chiang, S. Kahlal, J.-Y. Saillard and C. W. Liu, *Chem.–Eur. J.*, 2016, **22**, 9943–9947.

8 (*a*) H. Schmidbaur and A. Schier, *Angew. Chem., Int. Ed.*, 2015, **54**, 746–784; (*b*) H. Liu, C.-Y. Song, R.-W. Huang, Y. Zhang, H. Xu, M.-J. Li, S.-Q. Zang and G.-G. Gao, *Angew. Chem., Int. Ed.*, 2016, **55**, 3699–3703; (*c*) S. Li, X.-S. Du, B. Li, J.-Y. Wang, G.-P. Li, G.-G. Gao and S.-Q. Zang, *J. Am. Chem. Soc.*, 2018, **140**, 594–597; (*d*) R.-W. Huang, Y.-S. Wei, X.-Y. Dong, X.-H. Wu, C.-X. Du, S.-Q. Zang and T. C. W. Mak, *Nat. Chem.*, 2017, **9**, 689–697.

9 W. Liu and H. H. Thorp, *Inorg. Chem.*, 1992, **31**, 1585–1588.

10 R.-W. Huang, Q.-Q. Xu, H.-L. Lu, X.-K. Guo, S.-Q. Zang, G.-G. Gao, M.-S. Tang and T. C. W. Mak, *Nanoscale*, 2015, **7**, 7151–7154.

11 P. Pyykkö, *Chem. Rev.*, 1997, **97**, 597–636.

12 (*a*) H. G. V. Schnering and K. G. Hausler, *Rev. Chim. Miner.*, 1976, **13**, 71–81; (*b*) W. Beesk, P. G. Jones, H. Rumpel, E. Schwarzmann and G. M. Sheldrick, *J. Chem. Soc., Chem. Commun.*, 1981, 664–665; (*c*) C. Linke and M. Jansen, *Inorg. Chem.*, 1994, **33**, 2614–2616; (*d*) M. Jansen and C. Linke, *Angew. Chem., Int. Ed. Engl.*, 1992, **31**, 653–654.

13 (*a*) Y. Kikukawa, Y. Kuroda, K. Suzuki, M. Hibino, K. Yamaguchi and N. Mizuno, *Chem. Commun.*, 2013, **49**, 376–378; (*b*) Z.-Y. Wang, M.-Q. Wang, Y.-L. Li, P. Luo, T.-T. Jia, R.-W. Huang, S.-Q. Zang and T. C. W. Mak, *J. Am. Chem. Soc.*, 2018, **140**, 1069–1076.

14 I. Pastoriza-Santos and L. M. Liz-Marzan, *Pure Appl. Chem.*, 2000, **72**, 83–90.

15 S. Chen, L. Xiong, S. X. Wang, Z. Y. Ma, S. Jin, H. T. Sheng, Y. Pei and M. Z. Zhu, *J. Am. Chem. Soc.*, 2016, **136**, 10754–10757.

16 G. Li, Z. Lei and Q. M. Wang, *J. Am. Chem. Soc.*, 2010, **132**, 17678–17679.

17 (*a*) C. Yang, O. Elbjeirami, C. S. P. Gamage, H. V. R. Dias and M. A. Omary, *Chem. Commun.*, 2011, **47**, 7434–7436; (*b*) C.-M. Che, M.-C. Tse, M. C. W. Chan, K.-K. Cheung, D. L. Phillips and K.-H. Leung, *J. Am. Chem. Soc.*, 2000, **122**, 2464–2468; (*c*) D. Sun, L. L. Zhang, H. F. Lu, S. Y. Feng and D. F. Sun, *Dalton Trans.*, 2013, **42**, 3528–3532; (*d*) J. Jin, W.-Y. Wang, Y.-H. Liu, H.-W. Hou and Y.-T. Fan, *Chem. Commun.*, 2011, **47**, 7461–7463.

18 V. W.-W. Yam, V. K.-M. Au and S. Y.-L. Leung, *Chem. Rev.*, 2015, **115**, 7589–7728.